Study of Mechanical Properties of Membrane-Electrode Assemblies for Proton Exchange Membrane Fuel Cells By the Small-Punch Technique

ECS Transactions, 109 (9) 141-152 (2022)
10.1149/10909.0141ecst ©The Electrochemical Society

Study of Mechanical Properties of Membrane-Electrode Assemblies for Proton Exchange Membrane Fuel Cells By the Small-Punch Technique

Rebeca Hernández[a], Susana Merino[a], Gonzalo de Diego[a], Daniel Plaza[a], Luis Duque[b], M. Antonia Folgado[b], Antonio M. Chaparro[b], and Marta Serrano[a]

[a] Materials of Energy Interest, CIEMAT, Madrid 28040, Spain
[b] Low Temperature Fuel Cells, CIEMAT, Madrid 28040, Spain

Mechanical properties of membrane-electrode assemblies (MEAs) for proton exchange membrane fuel cells (PEMFCs) have been studied with the *small-punch* technique. MEAs were operated according to a non-accelerated aging protocol, with changes in humidification and cell temperature. After operation, degradation of the MEA is reflected by a decrease in power density, increase in the internal resistance, and decrease in open circuit voltage. Small disks (8 mm diam.) were taken from different locations of the degraded MEA to test the mechanical properties by small-punch. The results show an increase in plastic deflection and a decrease in maximum load of degraded MEAs, that result in lower apparent Young modulus. The degradation is larger in the area close to oxygen outlet. SEM microscopy shows that degradation affects majorly to the fibers of the carbon cloth gas diffusion layer (GDL). Combined small-punch and SEM correlate the change in mechanical properties on aged MEA with carbon fibers degradation. Such GDL degradation, probably together with the chemical degradation of the membrane, must be responsible for the increase in the internal resistance.

Introduction

The membrane-electrode assembly (MEA) suffers stressing conditions during operation in a fuel cell, due to harsh (electro-)chemical reactivity combined with mechanical stress induced by changes in the temperature, humidification, and static pressure (1),(2). Mechanical and chemical stresses may cause damage, leading to fragilization, cracks, tears, punctures, or pinhole blisters in the proton-exchange membrane (PEM) and/or the electrodes. Whereas chemical and electrochemical degradation processes have been extensively studied (see for instances (3) (4),(5)), the study of mechanical degradation is less explored. For this reason, techniques able to probe mechanical properties of MEAs are of high interest to better understand degradation processes and palliate their effects.

The mechanical properties of an MEA are composed of those of the membrane (PEM) and the two gas diffusion electrodes (GDEs). Both have been extensively characterized in the past. PEM properties depend on ambient parameters (temperature and relative humidity) and hydration state (6). Huang et al. found a reduction of MEA ductility of chemically aged and humidity cycled MEAs, attributed to constrained drying (7). They proposed the *strain-to-failure* as a metric for damage accumulation. Water

absorption decreases the Young's modulus of the PEM due to weakening of internal molecular interactions (8). The chemical degradation of the PEM has been related with the compression in the cell because of deformation energy activating chemical degradation processes (9). On the other hand, the mechanical strength of the electrodes resides principally in the properties of the gas diffusion layer (GDL), whereas the catalyst layer and microporous layers can be neglected. The GDL is composed of carbon fibers and a hydrophobic additive (PTFE) that comprise a porous layer of a few hundred micrometers of woven cloth or carbon paper. An intense experimental and theoretical research has been conducted towards mechanical properties responsible for the compressibility of the GDL and its effect on thickness, porosity, and permeability. Xiao et al. modelling on reconstructed GDL concludes that the frictional coefficient between fibers has more influence than mechanical properties of the fibers, and a preferential through plane displacement of fibers takes place upon compression (10).

A technique for the study of mechanical properties when the amount of material is limited, is the *small-punch*, that consists on the deformation of a disk with a 'small puncher', while recording the load (force) exerted by the puncher and the deflection produced on the disk (Fig. 1). Small-punch was originally developed by Handford Engineering Development Laboratory and by Massachusetts Institute of Technology, within the USA breeder and fusion programs in the late 70´s, to test transmission electron microscope (TEM) disks of a large number of irradiated alloys as a screening method to assess the sensitivity of creep and swelling to minor element composition changes (11). The main experimental result is a plot of load vs deflection that allows estimating mechanical strength, fracture toughness, impact, and tensile properties. The interesting singularity of this technique is that the disk specimen can be as small as a few millimeters, which makes it appropriate for localized studies of mechanical properties.

In this communication, small-punch is applied to the study of mechanical properties of MEAs with localized lateral resolution. It is an exploratory work to see the possibilities of the technique for MEA characterization, and, to our knowledge, the first study of this type. A comparative study of new and degraded MEAs is carried out, with determination of the accuracy limitations. Local mechanical properties of degraded MEAs are compared with SEM analysis and fuel cell response.

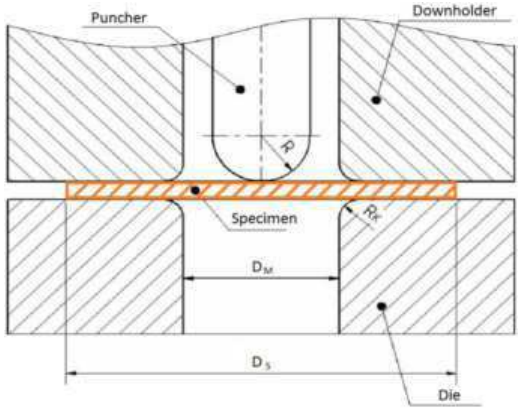

Figure 1. Scheme of the set-up for the small-punch technique.

Experimental

MEA assembly and testing

MEAs of 15 cm^2 active area were prepared from commercial electrodes with carbon cloth gas diffusion layer (ELAT GDE LT250EWALTSI, BASF, 0.25 mgPt cm^{-2}) and Nafion 212NR membrane (Ion Power, Dupont). The MEAs were assembled in PEMFC single cells using Au coated stainless-steel flow field plates, and 8 mm thickness stainless-steel end plates. One MEA was submitted to degradation by testing in single cells at 80 ^oC, under variable current loading, cell temperature, and humidification conditions, during 600 h (see below). During operation, polarization curves were obtained under standard conditions (80 ^oC, 100% RH, 1.5/3.0 stoichiometric H_2/O_2). Initial and final electrochemical active areas were measured with underpotential hydrogen adsorption/desorption technique at 30^oC, 100% RH, and 25 mV s^{-1} sweep rate, feeding with N_2/H_2 (30 ml min^{-1}/30 mil min^{-1}). The desorption peak charge was used for active area calculation.

Small-punch

Small-punch tests were performed according to the European standard BS EN 10371 that specifies the small punch method for testing metallic materials and the estimation of tensile, creep and fracture mechanical material properties (https://www.en-standard.eu/bs-en-10371-2021-metallic-materials-small-punch-test-method/). The experimental procedure is schematic in Fig. 1. Testing was carried under ambient conditions (22 ^oC and 30% RH) on MEA disks of 8 mm diameter taken from new and operated MEAs. Fig. 2 shows photographs of the MEA and disk samples.

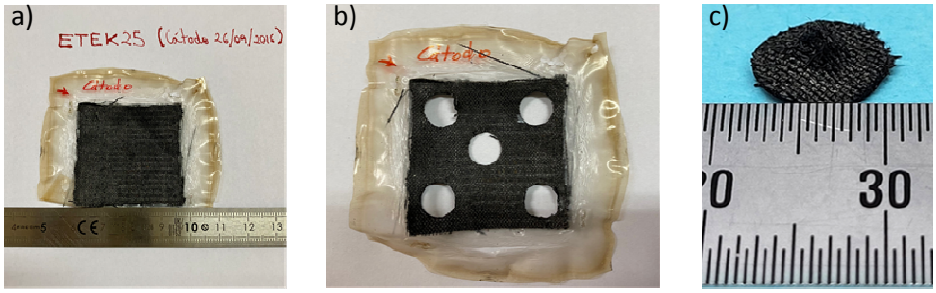

Figure 2. a) Degraded MEA after PEMFC single cell testing, b) after sampling, and c) single MEA disk after small-punch test.

The experimental result of the small-punch is a curve of the applied force against the deflection of the disk, as depicted in Fig. 3.

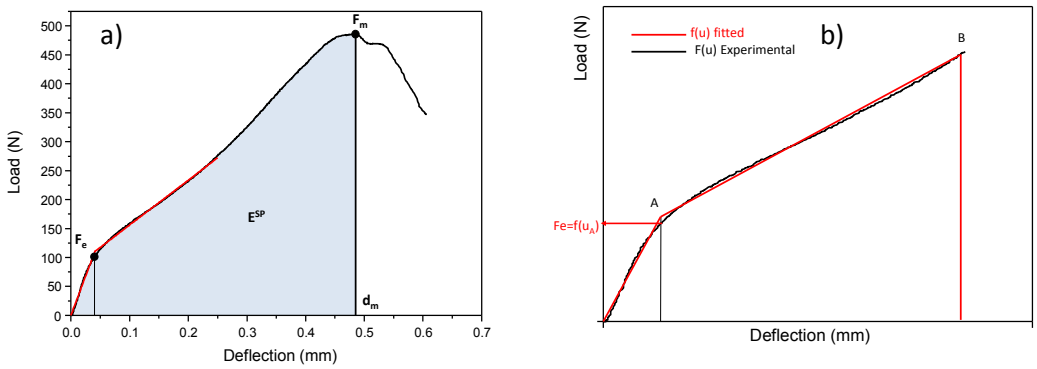

Figure 3. a) Load-deflection curve with characteristic parameters and b) calculation of Fe according to BS EN 10371.

The main parameters of the curve are the maximum load recorded during test (F_m, N); the load characterizing the transition from linearity to the stage associated with the spread of the yield zone through the specimen thickness (plastic bending stage) (F_e, N); the disk deflection at maximum load F_m (u_m, mm); and the fracture energy obtained from the area under the load punch displacement curve up to maximum load (E^{SP}, J).

Results and discussion

MEA testing

The MEAs were operated in single cells during 600 h under different conditions, including changes in current density (0 to 0.2 A cm^{-2}), humidification (RH= 0 and 100%), and temperature (40 to 80 ^{o}C), according to a non-accelerated aging profile which is highly stressing for the mechanical properties of the MEA. The complete operation history is plotted in Fig. 4, showing the time evolution of the input (thick lines) and output (thin lines) experimental parameters.

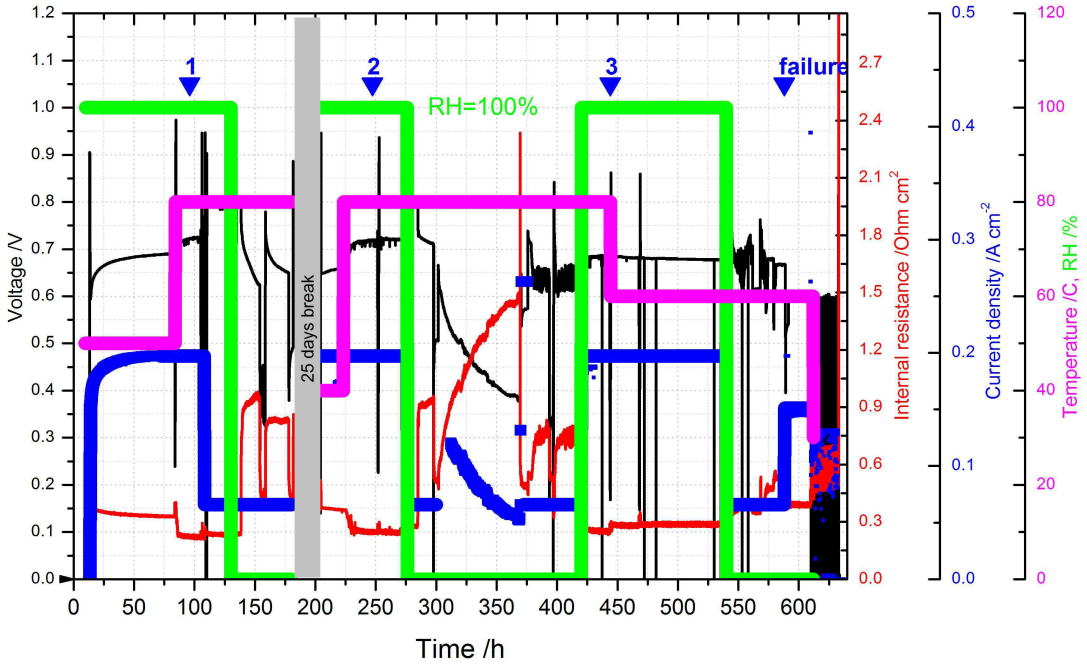

Figure 4. Parameters evolution of the MEA during testing. Input parameters (thick lines) are current density (blue), cell temperature (pink), and humidification (green). Output parameters (thin lines) are cell voltage (black), and internal resistance at 1 kHz (red). The cell was fed with H_2 (λ=1.5) and O_2 (λ=3.0) under 1 bar absolute pressure. Numbers 1-3 indicate the polarization curves in Fig. 5.

After the initial start-up period, lasting for first 75 h, the cell attains a steady-state with constant voltage and internal resistance at 1kHz ($R_{i,1kHz}$). A polarization curve was obtained afterwards (Fig. 5, curve 1). Then, the cell was operated at 80 ^{o}C and 0% RH during 50 h, after which the polarization curve 2 was measured (There is a break in this period where the cell was stopped and kept under N_2 for some days, so no change is expected in this time which is not considered in the temporal count of the experiment). Then, a third period of 150 h under 0 % RH and polarization curve 3 was obtained afterwards. As it is observed in Fig. 4, the operation under 0% RH and 80 ^{o}C is characterized by a significant increase in the internal resistance due to membrane and electrodes dryness that give rise to intense mechanical stress (7). After 530 h the cell was again brought to 0% RH, and this change gave rise to fatal failure after 585 h. Afterwards the cell was disassembled and the MEA characterized with small-punch and SEM.

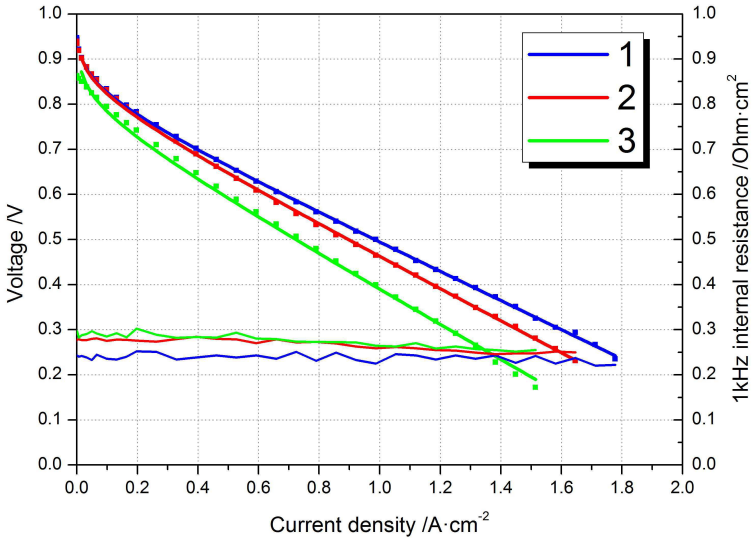

Figure 5. Polarization curves and internal resistance measured at 1 kHz of the MEA tested at different times (see Fig. 4). The curves were measured with H_2 (λ=1.5) and O_2 (λ=3.0) gas feeding, under and 1 bar_g backpressure, and 100 %RH.

Degradation caused by operation is reflected in the evolution of the polarization curves and internal resistances of Fig. 5. Quantitative information of the change in cell parameters can be obtained by fitting to the standard expression:

$$V = E - b \log(j/j_0) - j R_i \qquad [1]$$

Where V (V) is cell voltage, E (= 1.186 V) the thermodynamic potential, b (V dec^{-1}) the Tafel slope, j (A cm^{-2}) the cell current density, j_0 (A cm^{-2}) the exchange current density for oxygen reduction on Pt/C (12), and R_i (Ohm cm^2) the internal resistance. The parameter values are given in Table I together with experimental open circuit voltage (V_{oc}) and $R_{i,1kHz}$. The gradual decrease in V_{oc} reflects progressive short-circuiting of anode and cathode (ie. a direct path for electronic exchange being created during operation), together with the increase in cell resistance.

Short-circuiting is confirmed by the change observed in the cathodic voltammetries of Fig. 6, where the normal behavior at the beginning of life (BoL) changes to a thinner and positively tilted curve at end-of-life (EoL). Short-circuiting and probably also gas cross-over contribute to V_{oc} degradation as a consequence of membrane degradation (3). Another effect of the intense degradation is the brown color of water recovered from the cathode outlet.

Data in Table I also show the increase in the internal resistances, both Ri and $R_{i,1kHz}$, with operation time that must be ascribed to deterioration of high frequency current conduction processes, like the ionic conduction in the membrane and/or the electronic conduction in the electrodes. Summarizing, single cell characterization shows short-circuiting generation and resistance increase as the main effects of the degradation suffered by the MEA.

TABLE I. Tafel slope (b) and internal resistance (R_i) obtained from the fitting of polarization curves 1-3 of Fig. 3 to Eq. 1. Also shown history time (cf. Fig. 2), and experimental values of $R_{i,1kHz}$ (@ 0.2 A·cm^{-2}) and V_{oc} taken from Fig. 3.

Polarization curve	Time h	b V dec^{-1}	R_i Ohm cm^2	$R_{i,1kHz}$ Ohm cm^2	V_{oc} V
1	92	0.064	0.29	0.25	0.947
2	250	0.063	0.32	0.28	0.939
3	444	0.071	0.35	0.30	0.863

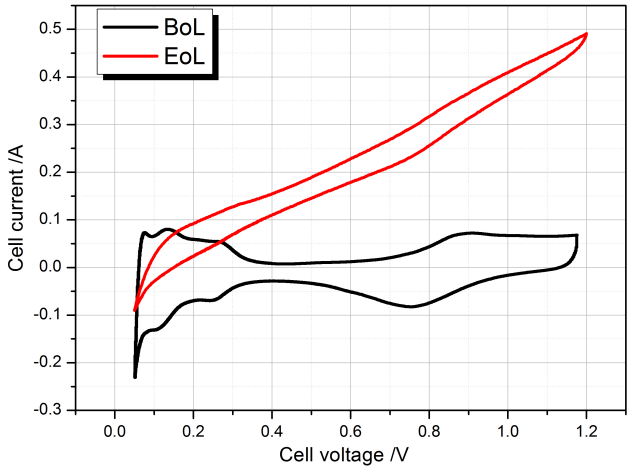

Figure 6. Cathode voltammetries taken at beginning-of-life (black), and end-of-life (red), under fully humidified H_2 (30 ml min^{-1}) and N_2 (30 ml min^{-1}) gas feeding in anode and cathode, respectively. Other conditions: 50 mV s^{-1} sweep rate, 30 ^{o}C cell temperature, and 1 bar backpressure.

Small-punch on new and degraded MEAs

Post-mortem study of the electrochemically degraded MEA was carried out with the small-punch technique in order to assess the impact of degradation on the mechanical properties. Results of the load vs. deflection curves are shown in Fig. 7 for MEAs before operation and after operation (cf. Fig. 4). Before operation, a dispersion of curves is obtained (N1 to N9 correspond to different samples) from which the experimental error of the procedure can be obtained.

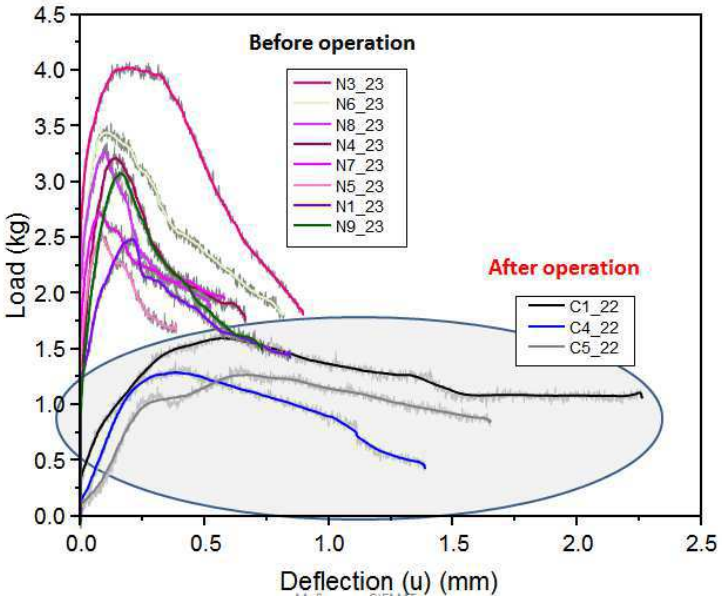

Fig. 7. Load vs deflection curves of MEAs disks before and after operation in a PEMFC (see Fig. 4 for operation history).

Small-punch testing on degraded MEAs is also shown in Fig. 7 on three locations of the MEA corresponding to the area close to oxygen inlet (C1), close to hydrogen inlet (C4) and at the outlet ports (C5) (see Fig. 8). Changes in the curves above the experimental error, when comparing new and degraded samples, reflect the degradation of mechanical properties of the MEAs on the different locations. The results of maximum load (F_m) and deflection at maximum load (u_m) are collected in Fig. 8 (see Fig. 3 for the meaning of these parameters). F_m decreases after degradation indicating a loss of strength. On the other hand, u_m increases on degraded samples, indicating softening of the material. So, both loss of strength and softening are the principal mechanical effects of MEA degradation.

Some more information can be obtained from the local degradation of the MEA. Whereas changes in the maximum load are below the experimental dispersion determined for this parameter, so no correlation can be found with the position in the cell, however the maximum deflection changes above experimental error and shows largest MEA softening close to the oxygen and hydrogen outlet ports. An apparent Young modulus (Y_{app}) can be obtained from the maximum load and deflection:

$$Y_{app} = F_m/u_m \qquad [2]$$

Y_{app} values are tabulated in Table II, showing a decrease by almost one order of magnitude on degraded MEAs. The decrease is larger in the position close to the gas exit ports (C5), where mechanical degradation appears to be more intense.

TABLE II. Results of the small-punch technique in non-operated and degraded MEA. For degraded MEA values are given in three local positions as indicated in Fig. 8.

Parameter	units	Non-operated	Operated		
		avg	C1	C4	C5
F_m	kN	30.1	15	12.5	11
u_m	mm	0.13	0.55	0.42	0.67
Y_{app}	kN mm^{-1}	231.5	27.3	29.8	16.4

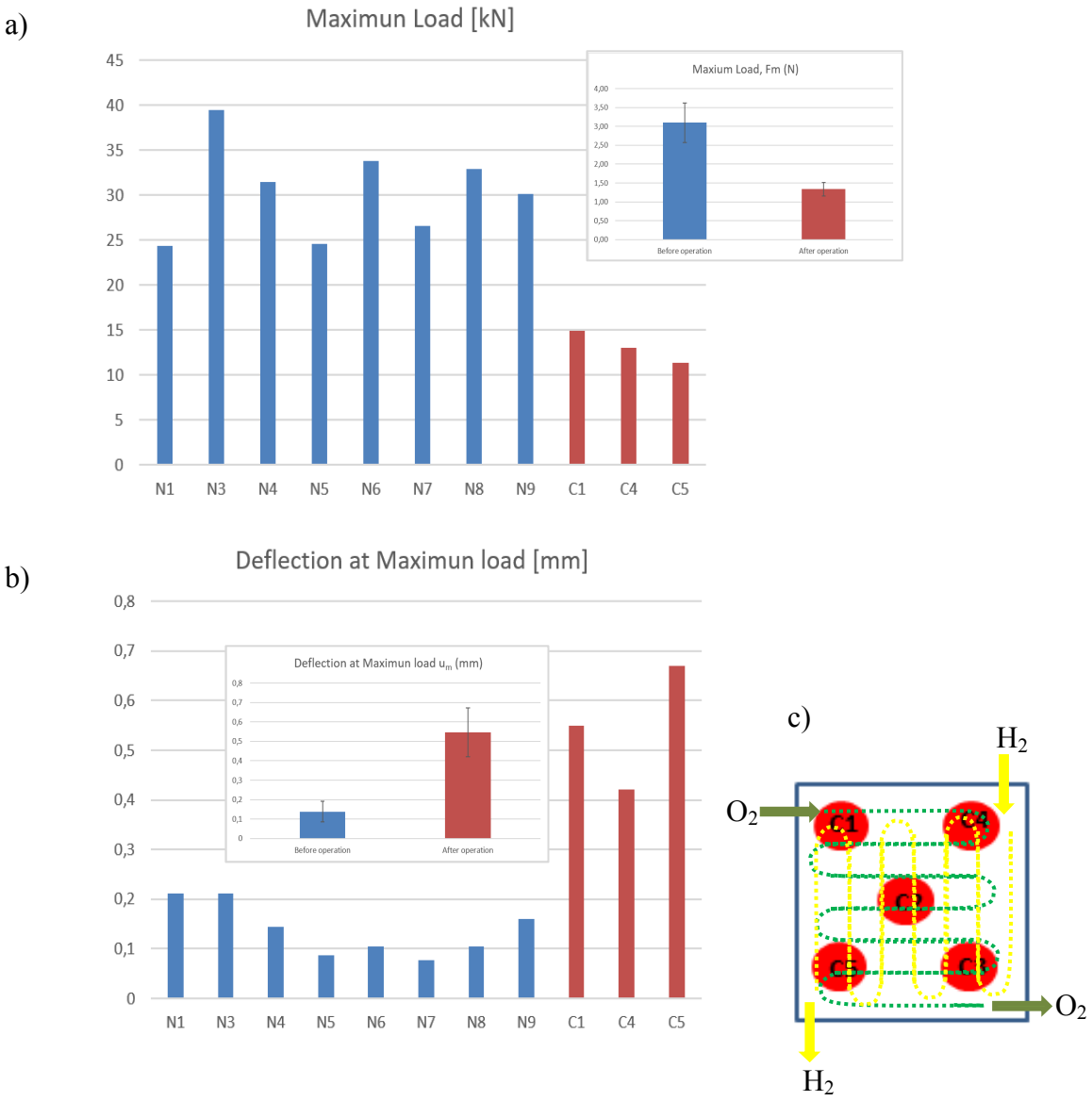

Fig. 8. Maximum load (a) and deflection at maximum load (b) of disks MEAs before and after operation. c) Scheme with localization of the disks from MEA in relation with oxygen and hydrogen paths in the cell.

Cross-section SEM analysis

Cross-section images of new and degraded samples are shown in Fig.9. The samples were metallographically prepared for cross section visualization, following a preparation methodology described in a previous work (13), on MEAs before and after cell operation. The main differences of operated samples are the lack of continuity of Pt layer and surface alteration (damage) produced in the carbon fibers of the GDL. Significantly, after the operation the fibers morphology change as a consequence of the increase in surface roughness and a sensitive decrease in the diameter.

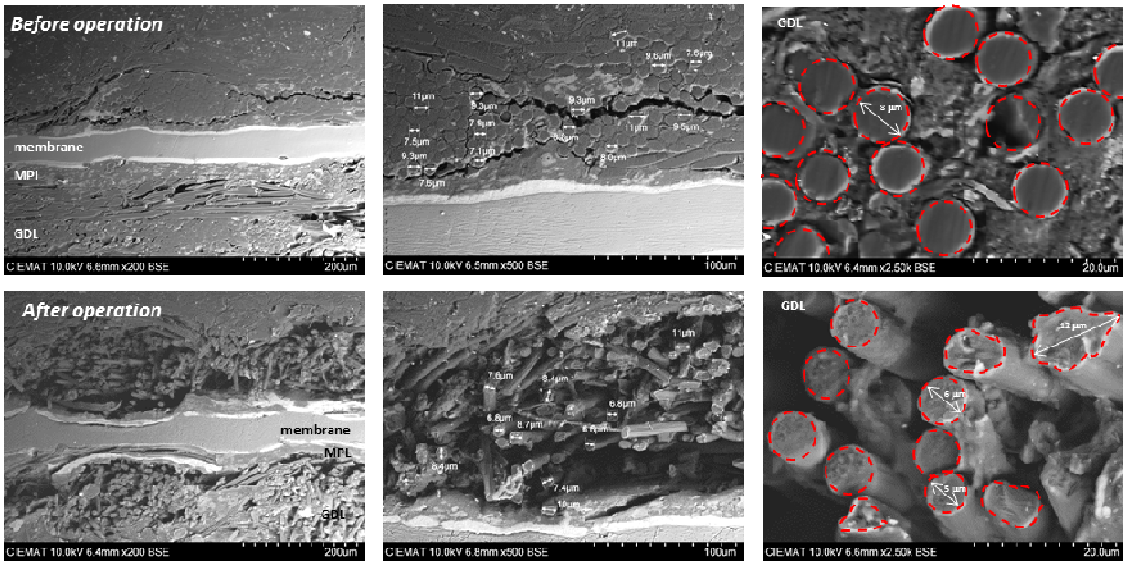

Figure 9: Cross sectional SEM images before and after operation showing fiber degradation.

Figure 10 shows SEM images of MEA samples after small-punch testing. They provide some more information about the degradation, by analyzing the effect of the small-punch load on the fibers and how they break. Whereas the new MEA shows a clean and homogeneous breaking of fibers, after degradation the thinner fibers of the GDL break elongated. The surface irregularities are evident if the degraded fibers. It can be concluded that the increase in maximum deflection on degraded samples observed by small-punch is a consequence of the degradation of the GDL fibers. Degradation of GDL fibers must be also most responsible for the (high frequency) internal resistance increase observed by degradation, together with the expected decrease in membrane conductivity on degraded MEA (3).

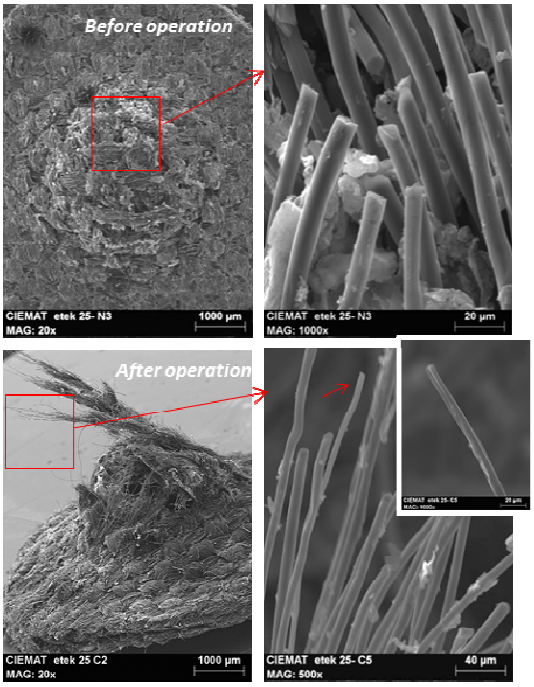

Figure 10. Small-punch sample after fracture showing the thinned fibers.

Conclusions

The small-punch technique is applied for the first time to the study of mechanical properties of MEAs of PEMFCs. Measurements are carried out on new and degraded MEAs after 600 h operation under changes in current, humidification, and temperature. The maximum load (F_{max}) and the elongation at maximum load (u_{max}) are the parameters identified to provide information on the degradation process, that can be combined in an apparent Young modulus (Y_{app}). It is found that the operating conditions described give rise to a softening of the MEAs, quantified by a sensitive decrease in Y_{app}. The mechanical degradation is more intense in MEA areas closer to the outlet ports of the cell. SEM observations show most intense degradation of the carbon fibers of the GDL.

Acknowledgements

This work was supported by the 'Ministerio de Ciencia, Innovación y Universidades' of Spain, Project ELHYPORT (PID2019-110896RB-I00).
(http://projects.ciemat.es/web/elhyport/presentacion).

References

1. Millichamp, J., Mason, T. J., Neville, T. P., Rajalakshmi, N., Jervis, R., Shearing, P. R. and Brett, D. J. L. Mechanisms and effects of mechanical compression and dimensional change in polymer electrolyte fuel cells - A review. *J. Power Sources* **284,** 305–320 (2015).
2. Hussein, A. I. and Zaidi, J. in *Polym. Membr. Fuel Cells* (eds. Zaidi, S. M. J. & Matsuura, T.) 1–431 (Springer Science, 2009). doi:10.1007/978-0-387-73532-0
3. Ramaswamy, N., Hakim, N. and Mukerjee, S. Degradation mechanism study of

perfluorinated proton exchange membrane under fuel cell operating conditions. *Electrochim. Acta* **53,** 3279–3295 (2008).

4. Borup, R. L., Kusoglu, A., Neyerlin, K. C., Mukundan, R., Ahluwalia, R. K., Cullen, D. A., More, K. L., Weber, A. Z. and Myers, D. J. Recent developments in catalyst-related PEM fuel cell durability. *Curr. Opin. Electrochem.* **21,** 192–200 (2020).
5. Pan, Y., Wang, H. and Brandon, N. P. Gas diffusion layer degradation in proton exchange membrane fuel cells: Mechanisms, characterization techniques and modelling approaches. *J. Power Sources* **513,** 230560 (2021).
6. Goulet, M. A., Khorasany, R. M. H., De Torres, C., Lauritzen, M., Kjeang, E., Wang, G. G. and Rajapakse, N. Mechanical properties of catalyst coated membranes for fuel cells. *J. Power Sources* **234,** 38–47 (2013).
7. HUANG, X., SOLASI, R., ZOU, Y., FESHLER, M., REIFSNIDER, K., CONDIT, D., BURLATSKY, S. and MADDEN, T. Mechanical Endurance of Polymer Electrolyte Membrane and PEM Fuel Cell Durability. *J. Polym. Sci. Part B Polym. Phys.* **44,** 2346–2357 (2006).
8. Lu, Z., Lugo, M., Santare, M. H., Karlsson, A. M., Busby, F. C. and Walsh, P. An experimental investigation of strain rate, temperature and humidity effects on the mechanical behavior of a perfluorosulfonic acid membrane. *J. Power Sources* **214,** 130–136 (2012).
9. Kusoglu, A., Calabrese, M. and Weber, A. Z. Effect of mechanical compression on chemical degradation of Nafion membranes. *ECS Electrochem. Lett.* **3,** 33–36 (2014).
10. Xiao, L., Luo, M., Zhang, H., Zeis, R. and Sui, P.-C. Solid Mechanics Simulation of Reconstructed Gas Diffusion Layers for PEMFCs. *J. Electrochem. Soc.* **166,** F377–F385 (2019).
11. Manahan, M. P. A New Postirradiation Mechanical Behavior Test—The Miniaturized Disk Bend Test. *Nucl. Technol.* **63,** 295–315 (1983).
12. Neyerlin, K. C., Gu, W., Jorne, J. and Gasteiger, H. A. Determination of Catalyst Unique Parameters for the Oxygen Reduction Reaction in a PEMFC. *J. Electrochem. Soc.* **153,** A1955 (2006).
13. Merino, S., Novillo, C., de Diego, G., Conde, J. J., Folgado, M. A., Ferreira-Aparicio, P. and Chaparro, A. M. Comparing Different Cross-Section Cutting Methods for SEM Analysis of Membrane-Electrodes Assemblies. *ECS Trans.* **92,** 87–94 (2019).